TOXICOLOGICAL SCIENCES **102(2)**, 241–253 (2008)
doi:10.1093/toxsci/kfm312
Advance Access publication January 3, 2008

A Biologically Based Dose-Response Model for Dietary Iodide and the Hypothalamic-Pituitary-Thyroid Axis in the Adult Rat: Evaluation of Iodide Deficiency

Eva D. McLanahan,* Melvin E. Andersen,† and Jeffrey W. Fisher*,[1]

*University of Georgia, Interdisciplinary Toxicology Program, Athens, Georgia 30602; and †The Hamner Institutes for Health Sciences, Division of Computational Biology, Research Triangle Park, North Carolina 27709

Received October 2, 2007; revised December 18, 2007; accepted December 24, 2007

A biologically based dose-response (BBDR) model was developed for dietary iodide and the hypothalamic-pituitary-thyroid (HPT) axis in adult rats. This BBDR-HPT axis model includes submodels for dietary iodide, thyroid-stimulating hormone (TSH), and the thyroid hormones, T_4 and T_3. The submodels are linked together via key biological processes, including (1) the influence of T_4 on TSH production (the HPT axis negative feedback loop), (2) stimulation of thyroidal T_4 and T_3 production by TSH, (3) TSH upregulation of the thyroid sodium (Na^+)/iodide symporter, and (4) recycling of iodide from metabolism of thyroid hormones. The BBDR-HPT axis model was calibrated to predict steady-state concentrations of iodide, T_4, T_3, and TSH for the euthyroid rat whose dietary intake of iodide was 20 μg/day. Then the BBDR-HPT axis model was used to predict perturbations in the HPT axis caused by insufficient dietary iodide intake, and simulation results were compared to experimental findings. The BBDR-HPT axis model was successful in simulating perturbations in serum T_4, TSH, and thyroid iodide stores for low-iodide diets of 0.33–1.14 μg/day. Model predictions of serum T_3 concentrations were inconsistent with observations in some cases. BBDR-HPT axis model simulations show a steep dose-response relationship between dietary intake of iodide and serum T_4 and TSH when dietary iodide intake becomes insufficient (less than 2 μg/day) to sustain the HPT axis. This BBDR-HPT axis model can be linked with physiologically based pharmacokinetic models for thyroid-active chemicals to evaluate and predict dose-dependent HPT axis alterations based on hypothesized modes of action. To support continued development of this model, future studies should include time course data after perturbation of the HPT axis to capture changes in endogenous iodide, serum TSH, T_4, and T_3.

Key Words: **iodide; BBDR model; HPT axis; thyroxine; TSH; pharmacokinetics.**

The hypothalamic-pituitary-thyroid (HPT) axis regulates many physiologic functions, including metabolism, growth, development, and reproduction. In humans, ingestion of insufficient or excessive amounts of dietary iodide, thyroid-active drugs, or exposure to thyroid-active environmental contaminants can perturb the HPT axis to varying degrees. If HPT alterations are severe enough or occur during a critical period of neurodevelopment, lifelong consequences may occur, such as learning deficits. Iodide deficiency, which leads to hypothyroidism, is the most preventable cause of mental retardation and brain damage throughout the world (Delange, 2001). Insufficient iodide intake is still prevalent in almost one-third of world population (Delange, 2001). Alterations in the HPT axis of laboratory animals are readily demonstrated using thyroid-active compounds or by altering the dietary intake of iodide (Brucker-Davis, 1998; Zoeller, 2007).

The process of thyroid hormone formation is highly regulated. The thyroid gland actively sequesters iodide via the sodium (Na^+)/iodide(I^-) symporter (NIS), which is an indispensable component of thyroid hormones. Iodide is then available for incorporation and use in thyroid hormone production. The normal thyroid gland produces thyroxine (T_4) in greater quantities than the biologically active hormone 3,5,3′-triiodothyronine (T_3) (Greer *et al.*, 1968). T_4 and T_3 are secreted from the thyroid gland into systemic circulation, where T_4 can be metabolized to T_3 in peripheral tissues by a family of enzymes called 5′-deiodinases. When circulating blood levels of T_4 and T_3 are low, the anterior pituitary gland produces more thyroid-stimulating hormone (TSH), a classical negative feedback loop. TSH, delivered by blood to the thyroid gland, binds to receptors on the plasma membrane of thyroid follicular cells. This receptor-TSH complex regulates second messenger cascades that stimulate thyroidal processes such as the increase in NIS expression and activity and increased production of thyroid peroxidase (TPO) and thyroglobulin (Tg) (Kogai *et al.*, 2006). These orchestrated biochemical events ultimately allow for compensatory increases in thyroidal uptake of iodide and production and secretion of T_4 and T_3.

Recently, several laboratories have reported on the potency of anions, which are environmental contaminants, to block thyroidal uptake of radiolabeled iodide in laboratory animals

[1] To whom correspondence should be addressed at 206 Environmental Health Sciences Department, University of Georgia, Athens, GA 30602-2102. Fax: (706) 542-7472. E-mail: jwfisher@uga.edu.

(perchlorate and nitrate, Tonacchera *et al*., 2004; Yu *et al*., 2002) and humans (perchlorate, Greer *et al*., 2002). The ability of perchlorate to alter the HPT axis in humans (e.g., increase serum TSH levels and decrease serum T_4 levels) appears to be feeble under conditions of high dietary iodide intake (Crump *et al*., 2000; Téllez *et al*., 2005) and significant for mildly iodide-deficient women (Blount *et al*., 2006). In this paper, a biologically based dose-response (BBDR) model for the HPT axis in the adult rat is developed to evaluate iodide deficiency as a first step in understanding the relationship between dietary iodide intake, potency of anions to block thyroidal uptake of dietary iodide, and disruption of the HPT axis.

Pharmacokinetic models have played an important role in understanding the quantitative aspects of the HPT axis. DiStefano and colleagues have published several kinetic papers on this topic. In particular, DiStefano *et al*. (1982) and DiStefano and Feng (1988) used a three-compartment rodent model for the thyroid hormones, T_4 and T_3, to estimate thyroid hormone production and metabolic clearance rates. Li *et al*. (1995) also used a compartmental approach to simulate the pulsatile release of TSH in humans. In 1996, Kohn *et al*. developed a rodent HPT axis submodel linked with a physiological model for 2,3,7,8-tetrachlorodibenzo-*p*-dioxin (TCDD) to evaluate TCDD-mediated induction of hepatic T_4 metabolism and clearance. More recently, Dietrich *et al*. (2002) described the negative feedback of the HPT axis in humans and the pulsatile secretion of TSH. Mukhopadhyay and Bhattacharyya (2006) also described the pulsatile secretion of TSH in humans using time delays to relate production of T_4 with TSH secretion. Physiologically based pharmacokinetic (PBPK) models for radiolabeled iodide (^{125}I) and perchlorate in rodents and humans have been developed for different life stages (Clewell *et al*., 2003a,b; Merrill *et al*., 2003, 2005) to evaluate the impact of perchlorate on thyroidal uptake of ^{125}I.

Although scientists have constructed compartmental models to describe the HPT axis, published models were not found that take into account TSH production and dietary iodide (^{127}I) linked to T_4 and T_3 formation and secretion. Thus, a quantitative BBDR-HPT axis model was developed to include the most informative serum hormones, namely, T_4 and T_3, and the signaling molecule, TSH, and dietary iodide. Features in the BBDR-HPT axis model include the active transport and regulation of iodide uptake into the thyroid by the NIS, T_4/TSH negative feedback loop, TSH stimulation of thyroidal processes, extrathyroidal metabolism of T_4 to form the biologically active T_3, and recycling of metabolically derived iodide from extrathyroidal metabolism of thyroid hormones.

MATERIALS AND METHODS

The BBDR-HPT axis submodels for the adult rat were constructed using simple model structures. The production of thyroid hormones (Equation 14) is controlled, in part, by the model predicted serum TSH concentration, and the maximal rate of active sequestration of iodide into the thyroid (Equation 2) is also controlled by the serum TSH concentration. This infers an instantaneous rate of change in protein synthesis without the use of delay functions or other equations to account for protein synthesis or degradation rates. This simple approach was adequate because BBDR-HPT axis model predictions were compared to experimental data under quasi steady-state conditions (days to months). This BBDR- HPT axis model was not validated against data to predict the initial onset of HPT axis disturbances for less than 24 h. Radiotracer time course data (supplementary data) were used to assist in obtaining preliminary parameter values for each subcompartment in the euthyroid adult rat. Other investigators have recently described endocrine systems, using serum levels of signaling molecules to control feedback loops such as the adult male rat hypothalamic-pituitary-gonadal (HPG) axis (Barton and Andersen, 1998) and the human HPG axis/menstrual cycle (Rasgon *et al*., 2003; Schlosser and Selgrade, 2000).

Models were coded using acslXtreme version 2.4.0.11 (Aegis Technologies, Huntsville, AL) and solved with the Gear algorithm for stiff systems. Standardized units of nanomoles (nmol), liters (L), kilograms (kg), and hours (h) were used in the submodels. The approach for the development of the BBDR-HPT axis model was to first create simple and independent submodel structures (supplementary data) for radiolabeled iodide, radiolabeled TSH, radiolabeled T_4, and radiolabeled T_3 using radiotracer studies reported in literature for the adult rat. This provided several BBDR-HPT axis model parameter values, although sometimes preliminary. Additional data pertaining to the metabolism and excretion of T_4 and T_3 were used to guide model development.

The submodels for iodide, TSH, T_4, and T_3 were linked as an interactive system to simulate the HPT axis in the euthyroid adult rat. The euthyroid steady-state BBDR-HPT axis model relied on dietary iodide as the only exogenous input. Finally, the calibrated euthyroid, iodide-sufficient adult rat BBDR-HPT axis model was tested for its ability to predict perturbations in the system under iodide-deficient conditions.

Submodel Structure and Key Equations

Iodide. Iodide was described as distributing into a volume of distribution (Vd) and thyroid gland (Fig. 1). Iodide is rapidly absorbed to the bloodstream from the digestive tract and quickly diffuses into extracellular spaces throughout the body. Iodide fate is largely determined by a competition between thyroidal sequestration and urinary excretion (Verger *et al*., 2001). Urinary excretion of iodide is described as a first-order clearance from the Vd. Uptake of iodide into the thyroid compartment is described assuming active uptake by the NIS and diffusion (Fig. 1).

Free iodide enters the thyroid in two ways as follows: (1) active uptake by NIS and (2) diffusion via ion channels. NIS is a plasma membrane protein that actively transports two sodium molecules with one iodide molecule down the sodium ion gradient generated by sodium-potassium ATPases (Kogai *et al*., 2006). TSH has been shown to stimulate NIS mRNA production, NIS protein expression, and retention in the plasma membrane (Carrasco, 1993; Kogai *et al*., 1997, 2000; Levy *et al*., 1997; Riedel *et al*., 2001; Sherwin and Tong, 1974). Sherwin and Tong (1974) found that TSH-induced stimulation of iodide transport increased the rate of iodide uptake and did not affect the affinity (Km_i) of iodide for the transporter. Thus, iodide uptake into the thyroid via the NIS ($r\mathrm{TNIS}_i$, nmol/h) and TSH-stimulated maximum NIS iodide transport rate ($\mathrm{VmaxT}_i^{\mathrm{TSH}}$, nmol/h) were described as follows:

$$r\mathrm{TNIS}_i = \frac{\mathrm{VmaxT}_i^{\mathrm{TSH}} \times \mathrm{Cvt}_i}{Km_i + \mathrm{Cvt}_i}, \quad (1)$$

$$\mathrm{VmaxT}_i^{\mathrm{TSH}} = \frac{\mathrm{Vmax}T_i \times \mathrm{Ca}_{\mathrm{TSH}}}{K_{\mathrm{NIS}}^{\mathrm{TSH}} + \mathrm{Ca}_{\mathrm{TSH}}}, \quad (2)$$

where Cvt_i (nmol/l) is the free concentration of iodide in thyroid blood, Km_i (nmol/l) is the affinity constant of iodide for the NIS, VmaxT_i (nmol/h) is the maximum rate of NIS iodide uptake, $\mathrm{Ca}_{\mathrm{TSH}}$ (nmol/l) is the serum concentration

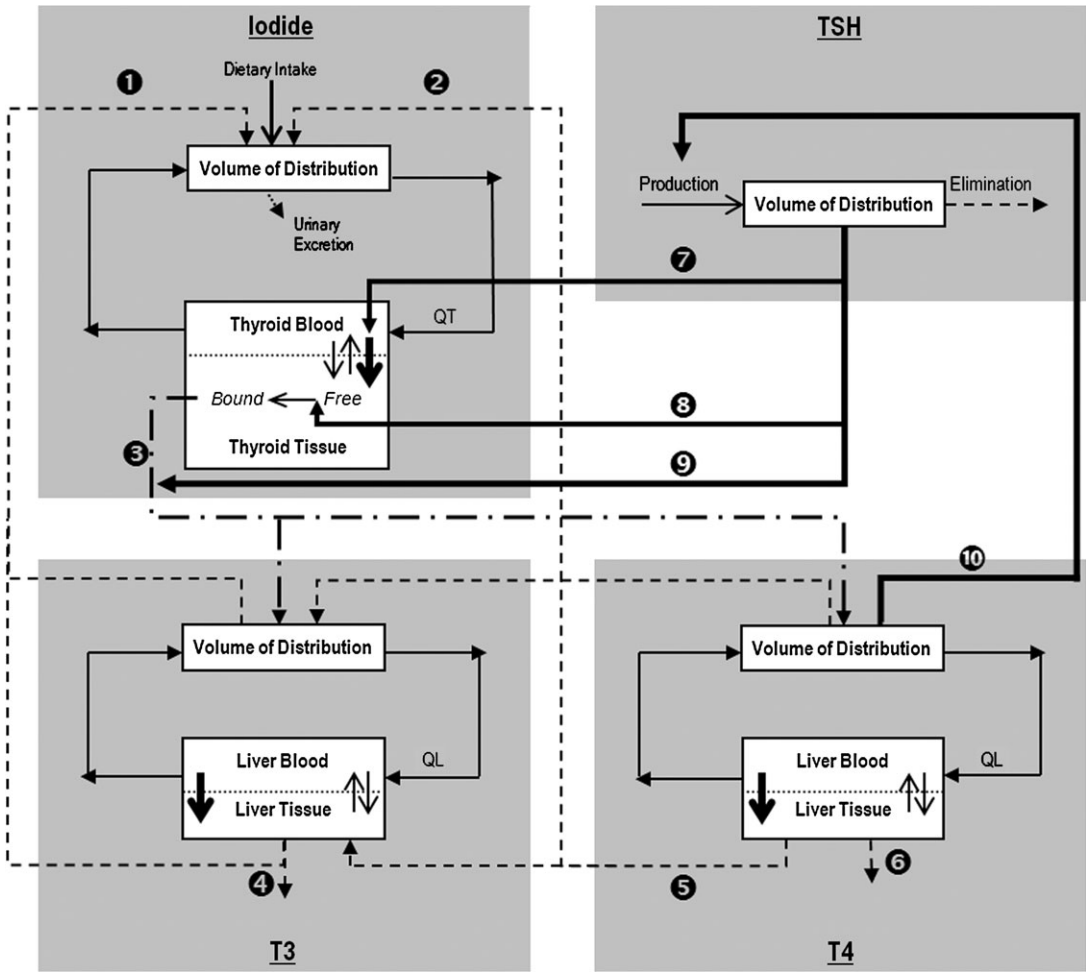

FIG. 1. BBDR-HPT axis model structure for the adult rat HPT axis is composed of submodels (shaded in gray) for dietary iodide, TSH, T_4, and T_3. Solid arrows (—►) represent blood flows, bold arrows (➔) within tissue compartments represent active uptake, diffusion limitation represented by solid arrows (→) within tissue compartments, metabolic links symbolized as dashed arrows (--►) between submodels. Dashed and dotted arrow (-·►) represents the use of dietary iodide in thyroid hormone production, and the bold (►) arrows connecting model processes show control (stimulation or inhibition) by the compound. Details shown in the figure are as follows: ❶ formation of free iodide from T_3 metabolism in the Vd and liver; ❷ formation of free iodide from T_4 to T_3 metabolism in the Vd and liver; ❸ loss of bound thyroidal iodide secreted as thyroid hormones; ❹ metabolism of T_3 (metabolism to free iodide and fecal elimination of T_3); ❺ deiodination of T_4 in the liver to T_3 and free iodide; ❻ phase II metabolism (conjugation of T_4) and excretion into feces; ❼ TSH stimulation of NIS iodide uptake; ❽ TSH stimulation of organification of iodide, forming thyroid hormone precursors; ❾ TSH stimulation of thyroid hormone production; ❿ T_4 negative feedback on TSH production.

of TSH, and K_{NIS}^{TSH} (nmol/l) is the serum concentration of TSH that results in half-maximal TSH stimulation of $VmaxT_i$.

Once iodide enters the thyroid by NIS-active uptake or diffusion, iodide is incorporated (organified) by binding to tyrosine residues present in Tg via a TPO-mediated mechanism (Degroot and Niepomiszcze, 1977). This bound fraction of iodide in this model represents the thyroidal iodide pool that is attached to Tg and the folding and formation of TH attached to the Tg backbone. TSH increases the expression of many genes involved in thyroid hormone synthesis, including Tg and TPO (Kogai *et al.*, 2006). The rate of incorporation of iodide (rIB, nmol/h) into thyroid hormone precursors and TSH stimulation ($VmaxB_i^{TSH}$, nmol/h) of the organification process is described by:

$$r\mathrm{IB} = \frac{\mathrm{VmaxB}_i^{\mathrm{TSH}} \times \mathrm{CTF}_i}{K\mathrm{b}_i + \mathrm{CTF}_i}, \tag{3}$$

$$\mathrm{VmaxB}_i^{\mathrm{TSH}} = \frac{\mathrm{VmaxB}_i \times \mathrm{Ca}_{\mathrm{TSH}}}{K\mathrm{b}_{\mathrm{TSH}} + \mathrm{Ca}_{\mathrm{TSH}}}, \tag{4}$$

where CTF_i (nmol/l) is the free concentration of iodide in the thyroid, Kb_i (nmol/l) is the concentration of free iodide in the thyroid when binding rate is half maximal, $VmaxB_i$ (nmol/h) is the maximum rate of organification of iodide, and Kb_{TSH} (nmol/l) is the concentration of serum TSH that results in half-maximal TSH stimulation of $VmaxB_i$.

Loss of free iodide from the thyroid by outward diffusion was described using an estimated permeability cross-product (PAT_i), and loss of bound iodide as thyroid hormones is described in Equations 14–16. Thus, the thyroid tissue compartment for iodide was described for free ($dATF_i/dt$, nmol/h), bound/thyroid hormone incorporated ($dATB_i/dt$, nmol/h), and total (AT_i, nmol) iodide by the following equations:

$$\frac{\mathrm{dATF}_i}{\mathrm{d}t} = r\mathrm{TNIS}_i + \mathrm{PAT}_i \times \left(\mathrm{Cvt}_i - \mathrm{CTF}_i\right) - r\mathrm{IB}, \tag{5}$$

$$\frac{\mathrm{dATB}_i}{\mathrm{d}t} = \left[r\mathrm{IB} - \left(r\mathrm{T4}_{\mathrm{prod}} \times \mathrm{T4}_i\mathrm{eq}\right) - \left(r\mathrm{T3}_{\mathrm{prod}} \times \mathrm{T3}_i\mathrm{eq}\right)\right], \tag{6}$$

$$AT_i = \int \frac{dATF_i}{dt} + \int \frac{dATB_i}{dt}, \quad (7)$$

where $rT4_{prod}$ is the secretion rate of T_4 from the thyroid (nmol T_4/h, Equation 16), $T4_ieq$ is the molar fraction of iodide in a T_4 molecule (0.6534), $rT3_{prod}$ is the secretion rate of T_3 from the thyroid (nmol T_3/h, Equation 15), and $T3_ieq$ is the molar fraction of iodide in a T_3 molecule (0.5848).

Thyroid-stimulating hormone (TSH), thyroxine (T_4), and 3,5,3′-triiodothyronine (T_3). TSH does not distribute into tissues, thus a one-compartment submodel for TSH was constructed using a Vd with a first-order clearance (Fig. 1). Each thyroid hormone submodel was developed with a Vd and liver compartment (Fig. 1). Bidirectional diffusion of T_4 in the liver was included in the description of hepatic influx and efflux. T_4 has also been shown to be actively transported into the liver by a high-affinity, low-capacity transporter, as well as a low-affinity, high-capacity transporter (Krenning *et al*., 1981). However, the rate of hepatic uptake of T_4 (rLU_{T4}, nmol/h) was simplified and described using a single Michaelis-Menten equation:

$$rLU_{T4} = \frac{Vmax_{T4}^{LU} \times \left(Cvl_{T4} \times 0.01\right)}{Km_{T4}^{LU} + \left(Cvl_{T4} \times 0.01\right)}, \quad (8)$$

where $Vmax_{T4}^{LU}$ is the maximal rate of active uptake of T_4 into the liver (nmol/h), Km_{T4}^{LU} is the affinity constant for T_4 active transport (nmol/l), and Cvl_{T4} is the concentration of T_4 in the liver venous blood (nmol/l). Since at least 99% of T_4 is bound to serum proteins in rodents (Mendel *et al*., 1992), the submodel code was modified to reflect only free-serum T_4 (1% of total serum T_4) available for active transport and diffusion into the liver. Phase II saturable metabolism of T_4 in the liver was described using Michaelis-Menten metabolism equations for glucuronidation (forming T_4-glucuronide, T_4-G) and type I 5′-deiodination of T_4 (forming T_3 and free iodide). The diffusion-limited liver blood compartment for T_4 was described using the equations:

$$\frac{dALb_{T4}}{dt} = Q_L \times \left(Ca_{T4} - Cvl_{T4}\right) + PAL_{T4} \times \left(CL_{T4} - \left(Cvl_{T4} \times 0.01\right)\right) - rLU_{T4}, \quad (9)$$

$$Cvl_{T4} = \frac{\int \frac{dALb_{T4}}{dt}}{V_{Lb} \times PL_{T4}}, \quad (10)$$

where $dALb_{T4}/dt$ is the rate of change of T_4 in the liver blood (nmol/h), Q_L is the blood flow to the liver (l/h), Ca_{T4} is the arterial blood concentration of T_4 perfusing the liver (nmol/l), PAL_{T4} is the liver permeability area cross-product for T_4 bidirectional diffusion (l/h), Cvl_{T4} is the concentration of T_4 in the liver venous blood (nmol/l), V_{Lb} is the volume of liver blood (l), and PL_{T4} is the T_4 liver:blood partition coefficient (unitless).

The liver tissue compartment for T_4 was described as follows:

$$\frac{dAL_{T4}}{dt} = PAL_{T4} \times \left(\left(Cvl_{T4} \times 0.01\right) - CL_{T4}\right) + rLU_{T4} - rDIL_{T4} - rUGT_{T4}, \quad (11)$$

$$CL_{T4} = \frac{\int \frac{dAL_{T4}}{dt}}{V_L}, \quad (12)$$

where dAL_{T4}/dt (nmol/h) is the rate of change of T_4 in the liver tissue, CL_{T4} (nmol/l) is the concentration of T_4 in the liver, rLU_{T4} (nmol/h, Equation 8) is the rate of active uptake of T_4 into the liver from liver blood, $rDIL_{T4}$ (nmol/h) is the Michaelis-Menten metabolic equation for rate of T_4 conversion to T_3 and free iodide by type I 5′-deiodinating enzymes, $rUGT_{T4}$ (nmol/h) is also a saturable Michaelis-Menten metabolism equation for the rate of formation of T_4-G formation, and V_L (l) is the volume of the liver. T_4 has also been shown to undergo other hepatic metabolic processes, such as sulfation (T_4-S formation), which accounts for a small fraction (6%) of overall T_4 metabolism (Rutgers *et al*., 1989), and T_4-S is rapidly deiodinated in the liver (Visser *et al*., 1990). To account for the rest of the body metabolism of T_4 to T_3, a first-order metabolism of T_4 was included as a loss from the Vd compartment.

Similar to T_4, transport of T_3 into the liver compartment was described by bidirectional diffusion and active uptake by a transporter protein (Fig. 1). Experimental evidence for hepatic transporter uptake of T_3 from blood suggests that T_3 uptake is not saturable at physiological conditions (Blondeau *et al*., 1988); thus, the active uptake was described as a first-order process. Hepatic metabolism of T_3 in the liver was also described as a first-order process, with the assumption that a percentage of the metabolized T_3 is excreted in feces as T_3 conjugates (T_3-G, T_3-S, etc.). The remainder is metabolized to free iodide, assuming T_3 metabolism to T_2 is the rate-limiting step in releasing free iodide. The fraction of T_3 metabolism excreted in feces (FT3feces, 0.30) was fit to provide an approximation (26%) of the percent dose of T_3 excreted in feces (4.9–54.9%; DiStefano and Sapin, 1987; DiStefano *et al*., 1993). First-order metabolism of T_3 was included in the Vd to account for rest of body metabolism of T_3 to T_0, also assuming that T_3 to T_2 is the rate-limiting step.

Linking the submodels to create a BBDR-HPT axis model. The submodels described in supplementary data for iodide, T_4, T_3, and TSH are linked as shown in Figure 1. All compartments for each submodel were assigned steady-state–derived masses at the onset of the simulations. The initial amounts of TSH, iodide, or thyroid hormones were established by running simulations to steady state with a dietary iodide intake of 20 μg/day. Dietary intake of iodide was assumed to take place over a 12-h period, with food/iodide consumption occurring during the night hours (7:00 P.M.–7:00 A.M.).

TSH is secreted by the anterior pituitary and is found in systemic circulation. Briefly, the TSH one-compartment model (described in supplementary data) in the linked BBDR-HPT axis model was modified to include an endogenous production term (Equation 13). The production of TSH is based on the primary negative feedback loop of the thyroid axis; that is, adequate levels of serum thyroid hormones result in a normal secretion of TSH from the pituitary, but when serum thyroid hormone levels decrease, the feedback control is diminished and TSH production rate increases. Several researchers have shown a negative correlation between serum T_4 and TSH concentrations (Fukuda *et al*., 1975; Pedraza *et al*., 2006; Riesco *et al*., 1977). This is a primary experimental observation reported by several laboratories and is used in the development of the negative feedback loop for the BBDR-HPT axis model. Since total serum T_4 is a common measurement in most thyroid disruptor studies, as opposed to free T_4, the TSH/T_4 negative feedback loop was described using total serum T_4 as shown in Equation 13. The empirical description of TSH production is regulated by the model-predicted total serum T_4 concentration (Ca_{T4}). The complete equation used to determine the amount of TSH in the Vd was as follows:

$$\frac{dAVd_{TSH}}{dt} = \underbrace{\frac{k_0^{TSH} \times K_{T4}^{inh}}{K_{T4}^{inh} + Ca_{T4}}}_{\text{production}} - \underbrace{kel_{TSH} \times Ca_{TSH}}_{\text{elimination}}, \quad (13)$$

where k_0^{TSH} (nmol/h) is the maximal production rate of TSH in the absence of T_4, K_{T4}^{inh} (nmol/l) is the estimated concentration of T_4 in the serum which results in half-maximal production rate of TSH, Ca_{T4} (nmol/l) is the total T_4 serum concentration, and Ca_{TSH} (nmol/l) is the TSH serum concentration calculated by dividing the integral of Equation 13 by Vd_{TSH} (l).

The rate of overall thyroidal production (release of T_4 and T_3 from Tg backbone—stored thyroidal iodide) and secretion of thyroid hormones (T_4 and T_3) were determined by a fitted rate constant (k_{TSH}^{IB}) times the model predicted serum concentration of TSH and concentration of available thyroidal iodide in the form of hormone precursors:

$$rTH_{prod} = k_{TSH}^{IB} \times Ca_{TSH} \times CTB_i, \quad (14)$$

where k_{TSH}^{IB} (l^2/nmol/h) is a linear rate term, Ca_{TSH} (nmol/l) is the serum concentration of TSH, and CTB_i (nmol/l) is the concentration of bound thyroidal iodide as thyroid hormone precursors. The proportion of thyroid hormones produced as T_3 and T_4 was then described as a fraction of the total production rate, using the following equations:

$$rT3_{prod} = FT3 \times rTH_{prod}, \quad (15)$$

$$rT4_{prod} = \left(1 - FT3\right) \times rTH_{prod}, \quad (16)$$

where $rT3_{prod}$ (nmol/h) is the rate of thyroidal T_3 production and $rT4_{prod}$ (nmol/h) is the rate of thyroidal T_4 production. The ratio of T_3/T_4 secretion increases during iodide deficiency. To account for this, Equation 17 was derived from Pedraza *et al*. (2006), who collected experimental data on total thyroidal iodide stores and thyroidal T_3/T_4 ratios for different iodide intake rates. FT3 (unitless) is the fraction of overall thyroid hormone production within the thyroid that is T_3 and was modeled as:

$$FT3 = 0.2652 \times AT^{-0.4684}, \quad (17)$$

where AT_i (μg) is the total amount of iodide in the thyroid, as calculated in Equation 7 and converted to micrograms. In iodide-deficient conditions, a shift from primarily T_4 to T_3 production in the thyroid occurs (Greer *et al*., 1968; Pedraza *et al*., 2006). This may be due to the increase in deiodination of T_4 in the thyroid or simply the formation of less T_4 because less iodide is needed to make T_3. However, no instances have been reported where the thyroid synthesizes only T_3 at the cost of zero T_4 production. A MIN command was implemented in acslXtreme to ensure that the exponential FT3 function (Equation 17) did not exceed 0.90.

Data sets used in steady-state euthyroid BBDR-HPT axis model calibration.

Serum T_4, and TSH, along with total thyroid iodide data from adult male Sprague-Dawley rats published by McLanahan *et al*. (2007) and serum T_3 data (unpublished data) from our laboratory were used to calibrate the model for steady-state euthyroid conditions in the adult rat (320 g). It was also important to include liver T_4 and T_3 concentrations for calibration; however, there are few data sets with tissue concentrations of thyroid hormones. Liver T_4 and T_3 concentrations reported by Morreale de Escobar *et al*. (1994) in euthyroid adult female Wistar rats were used in BBDR-HPT axis model calibration. Additionally, the only study found to report measured free iodide serum concentrations was Eng *et al*. (1999) who reported data for euthyroid (control) adult male Sprague-Dawley rats.

Model Parameters

Model parameters were derived from the published literature whenever possible. Default assumptions for allometric scaling were employed. Thus, blood flows (Q), maximum velocities (Vmax)[1] (An evaluation of literature for total thyroid iodide (^{127}I) concentrations for the range of body weights simulated in this study (120–500 g) showed slight change in total amount of thyroidal ^{127}I. The model parameter maintaining the stores in the thyroid is $VmaxBc_i$ (Vmax for iodide incorporation into thyroid hormone precursors). Thus, to empirically describe total thyroid ^{127}I concentrations, the value of $VmaxBc_i$ was divided by $BW^{0.75}$.), and permeability area cross-products (PA) were multiplied by body weight $(BW)^{0.75}$ and clearance rates (Cl and kel) were divided by $BW^{0.25}$. Volumes of distribution (Vd) were scaled linearly with BW.

Physiological parameters. Growth equations developed by Mirfazaelian *et al*. (2007) were used to account for body weight changes for simulations that were longer than 1 month. Otherwise, the terminal body weight reported for the study was used in simulation. Blood flows and tissue volumes (V) were obtained from literature (Brown *et al*., 1997; Malendowicz and Bednarek, 1986; McLanahan *et al*., 2007). Physiological parameters are shown in Table 1.

Literature-derived compound-specific parameters. When possible, compound-specific parameters for each submodel were derived from literature. Parameters for iodide, T_4, T_3, and TSH are shown in Table 2. Liver partition coefficients for T_4 (PL_{T4}, 1.27) and T_3 (PL_{T3}, 4.47) were determined from steady-state serum and liver concentrations reported by Escobar-Morreale *et al*. (1996) for female euthyroid, control rats. These values are similar to the values used by Kohn *et al*. (1996) for T_4 and T_3 liver partition coefficients (1.632 and 2.22, respectively) that were estimated from K_{ow} values and the use of various regression equations.

The Vd for T_4, T_3, and TSH were obtained from literature, as shown in Table 2, and the volume of the liver was subtracted from the Vdc for T_4 and T_3. The Vd for T_4 (Vdc_{T4}, 15.6% BW) was obtained from the thyroid hormone model developed by Kohn *et al*. (1996), whereas the Vd for T_3 (Vdc_{T3}, 18.6% BW) was used as estimated by DiStefano (1986) with a simple compartmental model for T_3. A TSH Vd (Vdc_{TSH}, 5.54% BW) was used as reported by Connors *et al*. (1984).

TABLE 1
Physiological Parameters for the Adult Rat[a]

Parameter	Value	Source
Tissue volumes		
Liver, VLc (% BW)	3.66	Brown *et al*. (1997)
Liver blood, VLBc (% VL)	21	Brown *et al*. (1997)
Thyroid, VTc (% BW)	0.005	McLanahan *et al*. (2007)
Thyroid blood, VTBc (% VT)	15.7	Malendowicz and Bednarek (1986)
Blood flows		
Cardiac output, QCc (l/h/kg$^{0.075}$)	14.0	Brown *et al*. (1997)
Liver, QLc (% QC)	17.4	Brown *et al*. (1997)
Thyroid, QTc (% QC)	1.6[b]	Brown *et al*. (1997)

[a]Body weight (BW, kg) is not shown in this table because body weights reported in each study were used in model simulations.
[b]Human value.

Clearance terms to account for metabolism in the Vd for TSH, T_4, and T_3 were calculated from literature values using the relationship

$$k_{el} = \frac{\ln 2}{t_{1/2}}, \quad (18)$$

where $t_{1/2}$ (h) is the serum half-life of the compound reported as 0.3667 h for ^{125}I-TSH (Lemarchand-Beraud and Berthier, 1981) and 6 and 12 h for T_3 and T_4, respectively (Abrams and Larsen, 1973).

Affinity constants, *K*m(s), for metabolism and active transport of iodide and T_4 were obtained from the literature (Table 2). The affinity constant for thyroid iodide transport by the NIS (Km_i) of 3.1×10^4 nmol/l was the average value reported by Gluzman and Niepomniszcze (1983), using radiolabeled iodide and euthyroid human and porcine thyroid cells. The affinity constant for active uptake of T_4 into the liver (Km_{T4}^{LU}) of 650 nmol/l was reported by Blondeau *et al*. (1988) using rat hepatocytes. Michaelis-Menten saturable metabolism of T_4 in the liver was described for the phase II glucuronidation and deiodination pathways. The saturable metabolism of T_4, by type I 5′-deiodination, was described assuming that one molecule of T_3 is formed and one molecule of free iodide is released for each molecule of T_4 metabolized. Phase II metabolism of T_4 (formation of T_4-G) occurs by a reaction catalyzed by uridine diphosphate glucuronyl transferases. The *K*m value for the type I 5′-deiodinase metabolism of T_4 (Km_{T4}^{DI}, 2300 nmol/l) was obtained from Leonard and Visser (1986) from *in vitro* metabolic studies, and the *K*m for the formation of T_4-G (Km_{T4}^{UGT}, 1×10^5 nmol/l) was taken from Visser *et al*. (1993) *in vitro* studies in Wistar rat liver microsomes. For each of these saturable metabolic processes, the *K*m values were derived from the literature, and Vmax values were optimized to fit serum kinetics of T_4 that resulted in values that were close to the literature reported radiotracer data for fraction of T_4 metabolized to T_3 (14–27%, DiStefano *et al*., 1982) and fraction of T_4 excreted in feces (10–38%, DiStefano and Sapin, 1987; Nguyen *et al*., 1993).

When submodels were combined to form the BBDR-HPT axis model, endogenous production of TSH was described as shown in Equation 13. The maximal rate of TSH production (k_0^{TSH}) was set to the maximum value (6 nmol/h) of TSH secretion reported by Connors *et al*. (1984) 14 days after thyroidectomy in adult female Sprague-Dawley rats (Table 2).

Parameter optimization. Model parameters not available in literature were first optimized to fit each radiotracer data set (^{125}I, ^{131}I-T_4, and ^{125}I-T_3, described in supplementary data); then when the models were linked to form the BBDR-HPT axis model, parameters were reoptimized to fit euthyroid, steady-state, iodide-sufficient (20 μg iodide/day) conditions. Volume of distribution for iodide (Vdc_i, 50% BW) and the linear rate term for thyroid

TABLE 2
Compound-Specific Parameters

Parameter	Value	Source
Volume of distribution (% BW)		
Iodide, Vdc_i	50[a]	Visual Fit
TSH, Vdc_{TSH}	5.54	Connors *et al.* (1984)
T_4, Vdc_{T4}	15.6[b]	Kohn *et al.* (1996)
T_3, Vdc_{T3}	18.6[b]	DiStefano (1986)
Partition coefficients (unitless)		
T_4—liver:blood, PL_{T4}	1.27	Escobar-Morreale *et al.* (1996)
T_3—liver:blood, PL_{T3}	4.47	Escobar-Morreale *et al.* (1996)
Permeability area cross-products (l/h/kg$^{0.75}$)		
T_4—liver blood to liver tissue, $PALc_{T4}$	0.0423	Optimized
T_3—liver blood to liver tissue, $PALc_{T3}$	0.1699	Optimized
Iodide—thyroid blood to thyroid tissue, $PATc_i$	0.0001	Merrill *et al.* (2003)
Affinity constants (nmol/l)		
Iodide—thyroid NIS, Km_i	31519	Gluzman and Niepomniszcze (1983); Merrill *et al.* (2003)
TSH—thyroid NIS, K_{TSH}^{NIS}	0.949	Optimized
Iodide—iodide organification in thyroid, Kb_i	244.59	Optimized
TSH—iodide organification in thyroid, Kb_{TSH}	733.98	Optimized
T_4—liver type I 5′-deiodinase, Km_{T4}^{DI}	2300	Leonard and Visser (1986)
T_4—liver glucuronidation, Km_{T4}^{UGT}	1×10^5	Visser *et al.* (1993)
T_4—liver uptake, Km_{T4}^{LU}	650	Blondeau *et al.* (1988)
Maximum velocities (nmol/h/kg$^{0.75}$)		
Iodide—thyroid NIS, $VmaxTc_i$	5738.267	Optimized
Iodide—iodide organification in thyroid, $VmaxBc_i$	1005.9[c]	Optimized
T_4—liver type I 5′-deiodinase, $Vmaxc_{T4}^{DI}$	19.89	Optimized
T_4—liver glucuronidation, $Vmaxc_{T4}^{UGT}$	3435.89	Optimized
T_4—liver uptake, $Vmaxc_{T4}^{LU}$	4384.73	Optimized
T_3—first-order liver uptake, km_{T3}^{LU} (l/h)	1.25	Optimized
Clearance values		
Iodide—urinary excretion, $ClUc_i$ (l/h/kg$^{0.25}$)	0.0046	Optimized
TSH—Vd clearance, $kelc_{TSH}$ (/h/kg$^{0.25}$)	1.8899	Lemarchand-Beraud and Berthier (1981)
T_4—Vd metabolism, $kelc_{T4}$ (/h/kg$^{0.25}$)	0.05[d]	Abrams and Larsen (1973)
T_3—Vd metabolism, $kelc_{T3}$ (/h/kg$^{0.25}$)	0.12[d]	Abrams and Larsen (1973)
T_3—liver metabolism, $kmetLc_{T3}$ (/h/kg$^{0.25}$)	3.65	Optimized
T_3—fraction of liver T_3 metabolism excreted in feces, FT3feces (unitless)	0.30	Visually Fit
TSH/thyroid hormone production parameters		
Thyroid hormone production constant, k_{TSH}^{IB} (l^2/nmol/h)	5×10^{-7}	Visually Fit
Maximum rate of TSH production in the absence of T_4, k_{TSH}^0 (nmol/h/kg$^{0.75}$)	6	Connors *et al.* (1984)
T_4 concentration for half-maximal TSH production, K_{inh_T4} (nmol/l)	0.2	Optimized

[a]Iodide Vd used in the model was calculated by subtracting VTc from Vdc_i.
[b]Vd for T_4 and T_3 were calculated by subtracting VLc from Vdc_{T4} and Vdc_{T3}, respectively.
[c]Scaled by dividing by $BW^{0.75}$. See footnote 1.
[d]Calculated from serum half-life using $kel = \ln 2/t_{1/2}$.

hormone production (k_{TSH}^{IB}, 5×10^{-7} l^2/nmol/h) were determined from visual fits. Global optimization was performed for model parameters in the BBDR-HPT axis model. During this optimization, all model parameters were optimized at steady state, for euthyroid and iodide-sufficient (20 μg I/day) conditions (serum and liver T_4 and T_3, serum TSH, serum-free iodide, and total thyroidal iodide). Additional data for metabolism were included in the optimization, as described previously. Optimization of model parameters was performed using acslXtreme Parameter Estimation version 2.4.0.11 (Aegis Technologies).

Model Performance Analysis

The predictive ability of the model was determined by calculating the area under the curve (AUC) ratios for each metric (serum T_4, serum T_3, serum TSH, and total thyroid iodide), as described by Gustafson *et al.* (2002). To determine the AUC predicted/measured (P/M) ratio, the BBDR-HPT axis model–predicted AUC was divided by the data-derived AUC for each of the four data sets (Figs. 2–4) tested under iodide-deficient conditions. The AUC P/M ratio calculation was:

$$\text{AUC P/M Ratio} = \frac{\text{AUC}_{\text{predicted}}}{\text{AUC}_{\text{experimental}}}, \quad (19)$$

where $AUC_{predicted}$ is the model-predicted AUC for serum T_4, T_3, TSH, or total thyroid iodide and $AUC_{experimental}$ is the corresponding data-derived AUC. Average AUC P/M ratios were calculated for each metric and overall model performance.

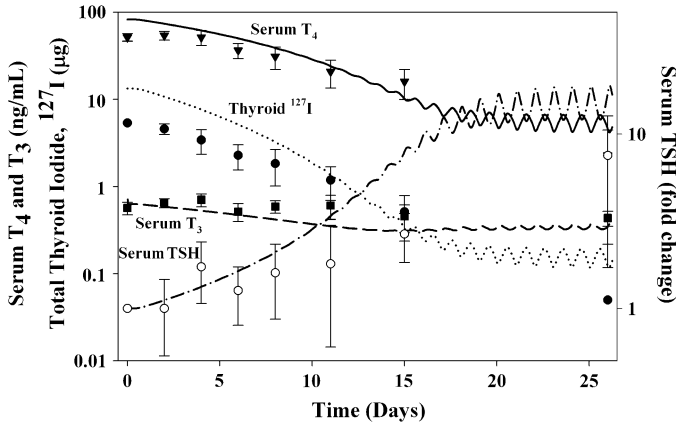

FIG. 2. Short-term effects of feeding a low iodide diet (0.35 μg I/day) on serum thyroid hormones and total thyroid iodide of adult male HSD rats. Rats began a low iodide intake of approximately 0.35 μg I/day on day 0 and continued for 26 days (Riesco *et al*., 1977). Model simulations are represented by lines for serum T_4 (——, ng/ml), T_3 (- - - -, ng/ml), TSH (– - –, fold change), and total thyroid ^{127}I (·····, μg). Data for serum T_4 (▼ ± SD), T_3 (■ ± SD), TSH (○), and total thyroid ^{127}I (● ± SD) were adapted from Riesco *et al*. (1977).

Sensitivity Analysis

An analysis of model parameter sensitivity under steady-state conditions was determined for predicted serum concentrations of T_4, T_3, and TSH and total thyroidal iodide content. Normalized sensitivity coefficients (NSCs) were calculated that represent a fractional change in output corresponding to a fractional change in the parameter (Clewell *et al*., 2000; Merrill *et al*., 2003; Tornero-Velez and Rappaport, 2001). Model parameters were increased by 1% and the model executed using iodide-sufficient (20 μg/day) and iodide-deficient (1 μg/day) intakes. The NSCs were calculated using the equation:

$$\text{Normalized sensitivity coefficient} = \frac{(A-B)/B}{(C-D)/D}, \qquad (20)$$

where A equals the model prediction (serum T_4, T_3, TSH, or total thyroid iodide) with a 1% increase in parameter value, B is model prediction with original parameter value, C is parameter value increased by 1%, and D is original parameter value.

Application of BBDR Model to Iodide Deficiency

Studies were available that provided weekly to monthly time-course information on iodide deficiency–induced HPT axis alterations (Okamura *et al*., 1981a,b; Riesco *et al*., 1977). In one case, recovery from iodide deficiency (Fukuda *et al*., 1975) was reported. These papers contained the most complete experimental data sets (iodide content of the diet, serum T_4, T_3, TSH, and total thyroid iodide). Many other studies prior to 1970 have been conducted; however, they were considered incomplete for modeling purposes. Average daily iodide intake was calculated by multiplying food consumption (20 g/day assumed when not reported for the study) by the iodide content in the diet (μg/g). To compare across studies, we have reported the intakes as micrograms iodide per day. The iodide deficiency data sets simulated using our BBDR-HPT axis model are briefly described below.

Riesco *et al*. (1977) provided adult male Holtzman-Sprague-Dawley (HSD) (120 g) rats a low iodide diet resulting in intake of 0.3–0.4 μg I/day for a short-term iodide deficiency study. They determined serum T_4, T_3, TSH, and total thyroid iodide after 0, 2, 4, 6, 8, 11, 15, and 26 days of feeding the low iodide diet. An average intake of 0.35 μg I/day was used in model simulation. A longer time course for HPT response of rats maintained on a low iodide diet was reported by Okamura *et al*. (1981a). Adult male Simonsen Albino (SA) and HSD rats were

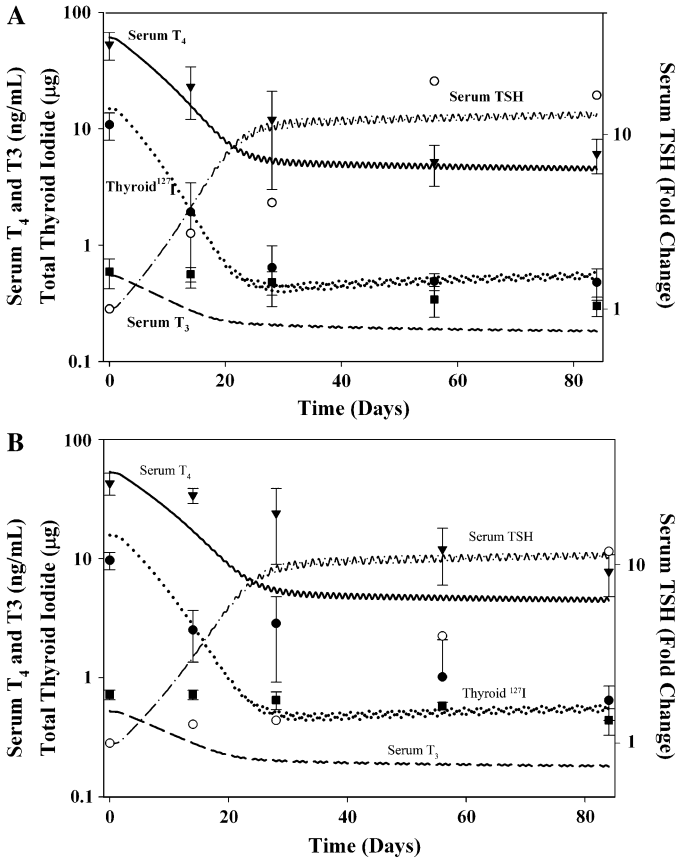

FIG. 3. Long-term effects of a low iodide diet (0.33 μg I/day) on serum thyroid hormones and total thyroid iodide of adult male (A) SA and (B) HSD rats. On day 0, rats began a low iodide intake of approximately 0.33 μg I/day and continued for 84 days (Okamura *et al*. 1981a). Model simulations are represented by lines for serum T_4 (——, ng/ml), T_3 (- - - -, ng/ml), TSH (– - –, fold change), and total thyroid ^{127}I (·····, μg). Data were adapted from Okamura *et al*. (1981a) for serum T_4 (▼ ± SD), T_3 (■ ± SD), TSH (○), and total thyroid ^{127}I (● ± SD).

divided by strain and provided a low iodide diet of 0.3–0.36 μg I/day (15–18 μg I/kg chow). Average intake of 0.33 μg I/day was used in model simulation. Measurements of serum T_4, T_3, TSH, and total thyroid iodide were obtained after 0, 14, 28, 56, and 84 days of feeding the low iodide diet. SA rats appeared to display a greater sensitivity or degree of HPT axis response to the low iodide diet than the HSD rats. In another study by Okamura *et al*. (1981b), they examined the opposing effects of iodide and nutritional deficiency, by administering two different low iodide diets (ICN Remington and Teklad Remington). The ICN Remington diet was not considered. Adult male HSD rats (139 g) were administered the Teklad Remington (57 ng I/g or 1.14 μg I/day, nutritionally adequate) diet and killed on days 19, 33, 63, and 96 of treatment for measurements of serum T_4, T_3, TSH, and total thyroid iodide. No baseline TSH levels were reported; thus, fold change in serum TSH levels were not used in this study. Fukuda *et al*. (1975) evaluated the recovery of the HPT axis in rats that were placed on iodide supplement after a low iodide diet. Adult male Sprague-Dawley rats (400–500 g) were placed on an iodide-deficient diet of 0.6 μg I/day (30 μg I/kg chow) for 7 months and then provided 2 or 8 μg I/day for 9 days in drinking water. The average iodide intake during the recovery period was 2.6 or 8.6 μg I/day. Serial blood samples were taken, and measurements of serum T_4 and TSH were obtained 0, 1, 2, 3, 6, and 9 days during supplementation. A wide range of serum TSH concentrations were observed at the onset of iodide supplementation, and some serum T_4 concentrations were reported as nondetectable. The data sets for the recovery period were expressed as percent of baseline.

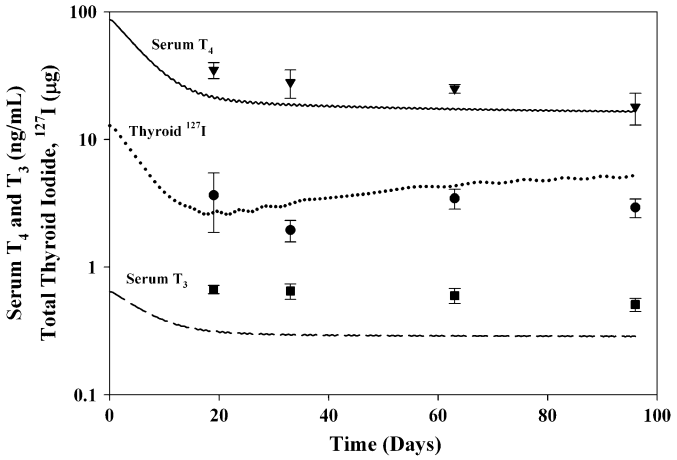

FIG. 4. Long-term effects of a low iodide diet (1.14 μg I/day) on serum thyroid hormones and total thyroid ^{127}I of adult male HSD rats. On day 0, rats were administered a low iodide diet providing 1.14 μg I/day and continued for 96 days (Okamura *et al*., 1981b). Model simulations are represented by lines for serum T_4 (——, ng/ml), T_3 (- - - -, ng/ml), and total thyroid ^{127}I (·····, μg). Data for serum T_4 (▼ ± SD), T_3 (■ ± SD), and total thyroid ^{127}I (● ± SD) were adapted from Okamura *et al*. (1981b).

RESULTS

Dietary Iodide BBDR-HPT Axis Model—Model Calibration and Simulation of Steady-State Euthyroid, Iodide-Sufficient Conditions

When the radiotracer submodels were linked to create the BBDR-HPT axis model by including the production of thyroid hormones (Equations 14–17), metabolism of thyroid hormones, recycling of freed iodide, and the T_4/TSH negative feedback loop (Equation 13), as shown in Figure 1, an adequate description of the euthyroid, steady-state iodide-sufficient (20 μg I/day) condition was not readily achieved. For example, predictions of serum iodide were too low, liver concentrations of T_3 and T_4 were too high, and serum T_4 concentrations were too high, which resulted in under-predicted serum TSH concentrations (simulations not shown). Therefore, the sub-model parameter values obtained to predict serum clearance kinetics of trace amounts of radiolabeled iodide, T_4, T_3, and TSH (supplementary data) were adjusted. This was not completely unexpected for describing endogenous masses of thyroid hormones, dietary iodide, and TSH. Thus, a global optimization of model parameters for the BBDR-HPT axis model was performed, and final model parameters are shown in Table 2. The calibrated steady-state euthyroid, iodide-sufficient model predictions for a 320-g rat are shown in Table 3. Total thyroid and free serum iodide, serum TSH, serum and liver T_4, and serum and liver T_3 model predictions fall within the range for normal rats reported in literature.

Iodide Deficiency HPT Axis Simulations

Using the BBDR-HPT axis model parameter values, globally optimized for euthyroid iodide-sufficient steady-state conditions, the ability of the model to predict temporal changes in serum thyroid hormones (T_4 and T_3), TSH, and total thyroidal iodide was tested for iodide-deficient conditions. HPT axis disturbances caused by feeding an iodide-deficient diet of 0.35 μg I/day for 26 days (Riesco *et al*., 1977) is depicted in Figure 2 for adult male HSD rats. Serum T_4 concentrations gradually decreased in a parallel fashion with thyroidal iodide stores, while only a slight change in serum T_3 concentrations occurred. Serum TSH concentrations increased over 10-fold during the study period. After 15 days of administration of the low iodide diet, the thyroidal iodide stores were severely depleted. The BBDR-HPT axis model predictions of serum thyroid hormones were in agreement with observed values. The predicted thyroidal iodide stores were slightly overpredicted initially and near the end of the study. Serum TSH increases were predicted during the first 11 days and then moderately overpredicted by day 15. In severe iodide-deficient conditions, when thyroidal iodide stores were predicted to be below 1 μg, oscillations in serum TSH and T_4 and thyroidal iodide occurred because of assumptions about dietary intake of iodide. Next, the capability of the BBDR-HPT axis model to predict changes during administration of 0.33 μg I/day administered for 84 days to adult male SA and HSD rats (Okamura *et al*., 1981a) was tested (Fig. 3). The SA strain (Fig. 3A) exhibited a greater sensitivity, shown by the rapid increase in TSH compared to the HSD strain (Fig. 3B). The BBDR-HPT axis model predicted the change in TSH better for the SA rats than the HSD rats. Serum T_3 concentrations were predicted to be lower than suggested by the data.

BBDR-HPT axis model simulations for an iodide-deficient diet of 1.14 μg I/day administered to adult male HSD (Okamura *et al*., 1981b) are depicted in Figure 4. The initial decrease in thyroidal iodide stores and the apparent recovery after 60 days suggests adaptive responses, such as the negative

TABLE 3
Steady-State Iodide-Sufficient Model Predictions Compared to Laboratory Data

HPT Axis Index	Units	Data ± SD	Model Predicted
Total thyroidal iodide	μg	15 ± 3[a]	17.5
Free serum iodide	μg/dl	7.3 ± 0.3, 10 ± 1.4[b]	9.7–15.6[c]
Serum T_4	ng/ml	40.6 ± 11.3[a]	39.4
Liver T_4	ng/g	18.7, 23.2, 25.5[d]	21.8
Serum T_3	ng/ml	0.46 ± 0.1[e]	0.46
Liver T_3	ng/g	3.7, 4.9, 5.7[d]	4.5
Serum TSH	ng/ml	6.5 ± 2.5[a]	6.3

[a]McLanahan et al. (2007).
[b]Eng et al. (1999).
[c]A range is reported because of the daily fluctuation predicted in serum iodide, resulting from the assumption that the rats consume chow 12 h of the 24-h day.
[d]Morreale de Escobar *et al*. (1994).
[e]Unpublished data.

feedback loop. The BBDR-HPT axis model predictions also suggest this as evidenced by an increase in predicted thyroidal iodide stores and little decline in serum thyroid hormones after 25 days. At a dietary intake of 1 μg/day, this strain of adult rat has some ability to compensate for low iodide intake. Predictions of serum T_3 were slightly underpredicted. Finally, the BBDR-HPT axis model was used to simulate recovery of the HPT axis in rats rendered iodide deficient for 7 months (Fukuda *et al*., 1975) with an average daily iodide intake of 0.6 μg/day (Fig. 5). On day 0 of the recovery phase, the rats were supplemented with iodide in drinking water to provide total intake of either 2.6 or 8.6 μg I/day. The BBDR-HPT axis model slightly overpredicted day 1 increases in serum T_4 following iodide supplementation for both doses, while the remaining predicted serum T_4 and TSH concentrations agreed with observations.

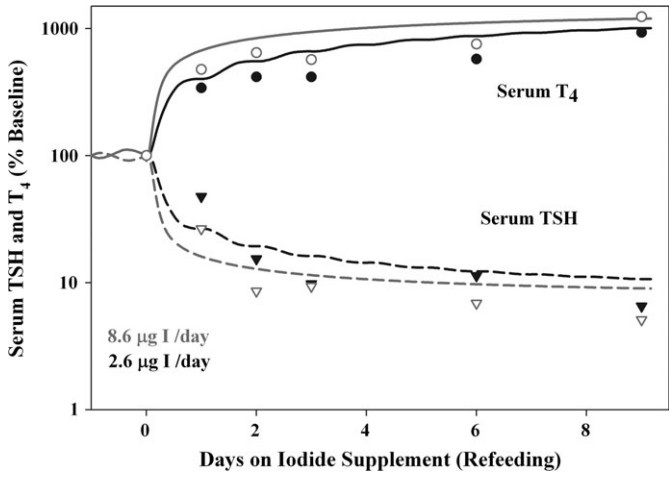

FIG. 5. Recovery from iodide deficiency in adult male Sprague-Dawley rats fed a low iodide diet for 7 months. After 7 months on a low iodide diet (0.6 μg I/day), rats were supplemented with iodide to provide total intake of approximately 2.6 μg I/day (black) or 8.6 μg I/day (dark gray) beginning on day 0 and continuing for 9 days (Fukuda *et al*., 1975). Model simulations of serum T_4 (solid lines) and TSH (dashed lines) are compared with recovery data modified from Fukuda *et al*. (1975) for serum T_4 (●, 2.6 μg I/day; ○, 8.6 μg I/day) and serum TSH (▼, 2.6 μg I/day; ▽, 8.6 μg I/day). Data expressed as percent of baseline recorded at day 0.

Model Performance Analysis

The predictive ability of the model to describe iodide deficiency was evaluated using AUC P/M ratios described by Gustafson *et al*. (2002). A value near 1.0 indicates agreement between model predictions and data observations. The AUC P/M ratios ranged from 0.37 to 2.27 for four metrics (serum T_4, T_3, TSH, and total thyroid iodide) across four iodide deficiency data sets (Figs. 2–4). The average AUC P/M ratios for each metric were 0.77, 0.54, 1.52, and 1.47 for serum T_4, T_3, TSH, and total thyroidal iodide, respectively. Taken together, the overall average AUC P/M ratio for the BBDR-HPT axis model predictive performance was 1.08.

Sensitivity Analysis

The sensitivity analysis of the BBDR-HPT axis model was carried out for steady-state serum concentrations of T_4, T_3, and TSH, and total thyroid iodide content for an iodide-sufficient intake of 20 μg I/day and iodide-deficient intake of 1 μg I/day. None of the parameters are associated with NSCs greater than 1.0, suggesting that there is minimal amplification of error from the inputs to the model outputs (Clewell *et al*., 2000). Total amount of thyroidal iodide predictions were most affected by a 1% change in the volume of the thyroid (VTc) (NSC = 0.99) under iodide-sufficient conditions and an NSC of 0.98 under iodide-deficient conditions. The parameters that play a major role in the retention of thyroidal bound iodide were more sensitive under iodide-sufficient conditions ($VmaxBc_i$, 0.94 and Kb_{TSH}, −0.93) for the prediction of total thyroid iodide than iodide-deficient conditions (both less than 0.01). A 1% change in the thyroid hormone production constant (k_{TSH}^{IB}) also reflected similar sensitivity of the total amount of iodide in the thyroid with NSCs of −0.95 and −0.96 under iodide-sufficient and -deficient conditions, respectively. Evaluation of the sensitivity analysis shows that the basal rate of TSH production (k_0^{TSH}) is more influential under iodide-deficient conditions (total thyroid iodide, NSC = −0.73; serum TSH, NSC = 0.89) than iodide-sufficient conditions (total thyroid iodide, NSC = 0.01; serum TSH, NSC = 0.49). Overall, serum T_4 and T_3 were much less sensitive than total thyroid iodide and serum TSH to a 1% change in model parameters.

DISCUSSION

The intent of this research was to develop a first generation BBDR model for the HPT axis in the adult rat using serum thyroxine (T_4) and TSH levels to control the TSH-mediated thyroidal uptake of dietary iodide and the production and secretion of thyroid hormones. This parsimonious approach represents the simplest model structure to describe the negative feedback loop and, for now, ignores protein synthesis rates. This approach was successful, with some exception, in describing HPT axis changes that occurred over days to months (steady-state conditions) for data sets from several laboratories. The dominant negative feedback control of T_4 on TSH was described (Equation 13), along with the stimulation of TSH on thyroidal iodide uptake (Equations 1–2) and subsequent thyroid hormone production (Equation 14).

Adult rats excrete approximately 95% of a daily iodide-sufficient intake (normal laboratory intake of 20 μg I/day) according to our model simulations. Urinary iodide levels arise from metabolism of thyroid hormones, as well as excess iodide provided in the diet. The normal adult rat stores 12–18 μg iodide (McLanahan *et al*., 2007), and model predictions estimate that rats utilize about 1.4 μg I/day in thyroid hormone production under normal, euthyroid conditions. Furthermore,

under iodide-sufficient conditions, our model predicts that 85% of the daily T_3 production is derived from T_4 metabolism, with the remaining (15%) produced in the thyroid. This is in agreement with others who suggest that at least 80% of the daily T_3 production occurs as a result of T_4 metabolism in a euthyroid system (Burger, 1986).

The BBDR-HPT axis model was tested for its ability to predict changes in serum T_4, T_3, TSH, and total thyroid iodide during administration of low iodide diets. The model predicted the temporal response (over days to months) for decreases in serum T_4 and increases in serum TSH resulting from the lack of available iodide for thyroid hormone production in an acceptable manner with some exceptions. Across all studies, the predictions of serum T_3 was less consistent with the experimental data compared to other predicted endpoints. However, our model does agree with literature data such that the percent of daily T_3 production in the thyroid increases significantly under iodide-deficient conditions (Abrams and Larsen, 1973; Greer *et al*., 1968). The percent of overall T_3 production in the thyroid is predicted to increase from 15% (iodide-sufficient 20 μg I/day intake) to 25% as iodide intake rate decreases to 1 μg/day and 45% at an iodide intake rate of 0.35 μg/day. Model predictions during steady-state iodide deficiency (1 μg I/day) suggest that the percent of daily iodide intake excreted in urine decreases to about 65% and only 0.67 μg of iodide is utilized in daily thyroid hormone production. Thyroid iodide stores are severely depleted to about 20% (2.8 μg) of euthyroid, iodide-sufficient values, resulting in a decrease of over 50% in serum T_4 concentrations.

Using the BBDR-HPT axis model to evaluate dietary intake of iodide under steady-state conditions, a sharp decline in serum T_4 is predicted to occur when dietary intake is less than 2 μg I/day even in the presence of significant TSH stimulation of the thyroid (Fig. 6). Others have reported that laboratory rats require an iodide intake greater than 2 μg I/day to maintain euthyroid status (Pedraza *et al*., 2006).

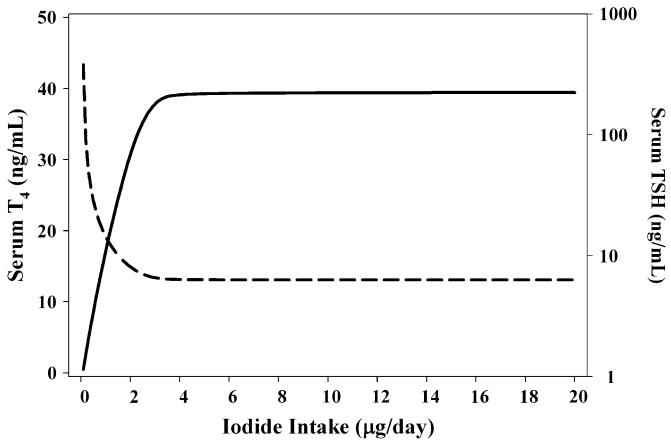

FIG. 6. Iodide dose-response plot for serum T_4 and TSH. BBDR-HPT axis model was used to determine steady-state serum T_4 and TSH concentrations over a wide range of iodide intakes, intakes ranged from insufficient (0–2 μg I/day) to sufficient (> 2 μg I/day).

Comments on the First-Generation BBDR-HPT Axis Model

Several feature of the HPT axis were not included in the present model, for example, protein synthesis, thyroid-releasing hormone (TRH), or metabolites of thyroid hormones (reverse T_3, T_2, T_1, or thyroid hormone conjugates other than T_4-glucuronide). Physiological changes were not included that occur during long-term iodide deficiency and hypothyroidism. For example, structural changes in the thyroid (Colzani *et al*., 1999), increases in thyroid blood flow (Michalkiewicz *et al*., 1989), and altered biological activity of thyroid hormone–metabolizing enzymes (Janssen *et al*., 1994; Obregon, *et al*., 2005; Pedraza *et al*., 2006) were not accounted for in this model iteration. TRH, secreted by the hypothalamus, stimulates release of TSH from the pituitary, while circulating T_4 and T_3 inhibit both TRH and TSH synthesis and release (Fail *et al*., 1999; Simpkins *et al*., 1976). Our model does not explicitly describe TRH effect on TSH; however, the BBDR-HPT axis model relates serum T_4 levels to the TSH output from the pituitary, which implicitly includes TRH effects. There are no time-course data for TRH changes under iodide deficiency or following exposure to thyroid active compounds; thus, it is not possible to adequately describe TRH mathematically for euthyroid, steady-state or perturbed systems.

A challenge in the development of this model was relying on published HPT axis data sets that varied dramatically. For example, reported TSH values for adult male Sprague-Dawley rats range from 4.6 ± 0.49 ng/ml to 8.73 ± 0.81 ng/ml (McLanahan *et al*., 2007), approximately 15–20 ng/ml (Siglin *et al*., 2000), 327 ± 174 ng/ml (Okamura *et al*., 1981a), to a high of 440 ± 220 ng/ml (Lemarchand-Beraud and Berthier, 1981). Several factors may contribute to this variability including, time of sampling, weight of animal, and radioimmunoassay analytical method, and standards employed. Thus, in reporting our model results, we reported TSH as fold change to normalize and compare model simulations with more data sets. Most of the iodine deficiency studies occurred prior to 1990, and many methods for analysis of thyroid hormones, TSH, and iodide have evolved since their publication. Another significant concern is verification of iodide and iodine in the rat chow. This amount can vary significantly between batches of rodent chow (Naeije *et al*., 1978). Unfortunately, the actual iodide and iodine concentrations in rodent chow is not usually measured by laboratories.

The development of this model was initiated with the ultimate goal of integrating it with PBPK models for thyroid toxicants to interpret dose-response characteristics of HPT axis–mediated toxicity. Thyroid toxicants are defined as compounds, which alter serum thyroid hormone and TSH concentrations (Zoeller and Tan, 2007). The role of dietary iodide intake and the ability of anions to disturb the HPT axis will be explored with this first generation model and then

expanded to include thyroid active chemicals that act by other modes of action.

Future studies to support continued development of the BBDR-HPT axis model should include time-course studies after perturbation of the HPT axis to capture changes in endogenous iodide, serum TSH, T_4, and T_3, and thyroid hormones in tissues, such as the liver and regions of the brain. Time scales for intra- and extrathyroidal changes in protein synthesis and activity need to be explored in further detail. To this end, Kogai *et al.* (1997) have demonstrated that changes in NIS mRNA in FRTL-5 cells occur much faster (6 h) than protein expression (36 h) in response to TSH exposure. *In vitro* studies are also needed to better understand endogenous synthesis rates of TSH and thyroid hormones and metabolic clearance rates.

SUPPLEMENTARY DATA

The supplementary data includes details of the radiotracer submodel development for ^{125}I, ^{125}I-TSH, ^{125}I-T_3, and ^{131}I-T_4, as well as model simulations for these stand alone submodels. The submodels developed and presented in supplementary data were used to test the model structure and obtain preliminary model parameters for the linked BBDR-HPT axis model. The model parameters optimized for radiotracer submodels (Table 1S) were used with the model structures depicted in Figure 1S for simulations shown in Figure 2S. These model parameters were reoptimized to euthyroid, steady-state iodide-sufficient conditions in the dietary iodide BBDR-HPT axis combined model. Supplementary data are available online at http://toxsci.oxfordjournals.org/.

FUNDING

United States Environmental Protection Agency Science to Achieve Results research grant (RD83213401-0); United States Environmental Protection Agency Science to Achieve Results Fellowship (FP-91679301-0 to E.D.M).

ACKNOWLEDGMENTS

The authors extend special thanks to Dr Kyung O. Yu for providing experimental data sets for use in radioiodide model development. Sincere thanks to Dr Jerry L. Campbell, Jr, for model review. The views expressed in the manuscript are those of the authors and do not represent official opinions of the United States Environmental Protection Agency. Mention of trade names or commercial products does not constitute endorsement or recommendation for use.

REFERENCES

Abrams, G. M., and Larsen, P. R. (1973). Triiodothyronine and thyroxine in the serum and thyroid gland of iodine-deficient rats. *J. Clin. Invest.* **52,** 2522–2531.

Barton, H. A., and Andersen, M. E. (1998). A model for pharmacokinetics and physiological feedback among hormones of the testicular-pituitary axis in adult male rats: A framework for evaluating effects of endocrine active compounds. *Toxicol. Sci.* **45,** 174–187.

Blondeau, J., Osty, J., and Fracon, J. (1988). Characterization of the thyroid hormone transport system of isolated hepatocytes. *J. Biol. Chem.* **263,** 2685–2692.

Blount, B. C., Pirkle, J. L., Osterloh, J. D., Valentin-Blasini, L., and Caldwell, K. L. (2006). Urinary perchlorate and thyroid hormone levels in adolescent and adult men and women living in the United States. *Environ. Health Perspect.* **114,** 1865–1871.

Brown, R., Delp, M., Lindstedt, S., Rhombert, L., and Belies, R. (1997). Physiological parameter values for physiologically based pharmacokinetic models. *Toxicol. Ind. Health.* **13,** 407–484.

Brucker-Davis, F. (1998). Effects of environmental synthetic chemicals on thyroid function. *Thyroid* **8,** 827–856.

Burger, A. (1986). Nondeiodinative pathways of thyroid hormone metabolism. In *Thyroid Hormone Metabolism.* (G. Hennemann, Ed.), pp. 255–276. Marcel Dekker., Inc, New York.

Carrasco, N. (1993). Iodide transport in the thyroid gland. *Biochimica et Biophysica Acta* **1154,** 65–82.

Clewell, III, H. J., Gentry, P. R., Covington, T. R., and Gearhart, J. M. (2000). Development of a physiologically based pharmacokinetic model of trichloroethylene and its metabolites for use in risk assessment. *Environ. Health Perspect.* **108**(Suppl), 283–305.

Clewell, R. A., Merrill, E. A., Yu, K. O., Mahle, D. A., Sterner, T. R., Fisher, J. W., and Gearhart, J. M. (2003a). Predicting neonatal perchlorate dose and inhibition of iodide uptake in the rat during lactation using physiologically-based pharmacokinetic modeling. *Toxicol. Sci.* **74,** 416–436.

Clewell, R. A., Merrill, E. A., Yu, K. O., Mahle, D. A., Sterner, T. R., Mattie, D., Robinson, P., and Fisher, J. W. (2003b). Predicting fetal perchlorate dose and inhibition of iodide kinetics during gestation: A physiologically-based pharmacokinetic analysis of perchlorate and iodide kinetics in the rat. *Toxicol. Sci.* **73,** 235–255.

Colzani, R. M., Alex, S., Fang, S.-L., Stone, S., and Braverman, L. E. (1999). Effects of iodine repletion on thyroid morphology in iodine and/or selenium deficient rat term fetuses, pups, and mothers. *Biochimie* **81,** 485–491.

Connors, J. M., DeVito, W. J., and Hedge, G. A. (1984). The effects of the duration of severe hypothyroidism and aging on the metabolic clearance rate of thyrotropin (TSH) and the pituitary TSH response to TSH-releasing hormone. *Endocrinology* **114,** 1930–1937.

Crump, C., Michaud, P., Téllez, R., Reyes, C., Gonzalez, G., Montgomery, E. L., Crump, K. S., Lobo, G., Becerra, C., and Gibbs, J. P. (2000). Does perchlorate in drinking water affect thyroid function in newborns or school-age children? *J. Occup. Environ. Med.* **42,** 603–612.

Delange, F. (2001). Iodine deficiency as a cause of brain damage. *Postgrad. Med. J.* **77,** 217–220.

Degroot, L. J., and Niepomiszcze, H. (1977). Biosynthesis of thyroid hormone: Basic and clinical aspects. *Metabolism* **26,** 665–718.

Dietrich, J. W., Tesche, A., PIckardt, C. R., and Mitzdorf, U. (2002). Fractal properties of the thyrotropic feedback control: Implications of a nonlinear model compared with empirical data. In: *Cybernetics and Systems 2002*. R. Trappl (Hrsg), Vienna.

DiStefano, III, J. J. (1986). Modeling approaches and models of the distribution and disposal of thyroid hormones. In *Thyroid Hormone Metabolism* (G. Hennemann, Ed.), pp. 39–76. Marcel Dekker, Inc., New York.

DiStefano, III, J. J., and Feng, D. (1988). Comparative aspects of the distribution, metabolism, and excretion of six iodothyronines in the rat. *Endocrinology* **123,** 2514–2525.

DiStefano, III, J. J., Malone, T., and Jang, M. (1982). Comprehensive kinetics of thyroxine distribution and metabolism in blood and tissue pools of the rat

from only six blood samples: Dominance of large, slowly exchanging tissue pools. *Endocrinology* **111,** 108–117.

DiStefano, III, J. J., Nguyen, T. T., and Yen, Y. (1993). Transfer kinetics of 3,5,3′-triiodothyronine and thyroxine from rat blood to large and small intestines, liver, and kidneys *in vivo*. *Endocrinology* **132,** 1735–1744.

DiStefano, III, J. J., and Sapin, V. (1987). Fecal and urinary excretion of six iodothyronines in the rat. *Endocrinology* **121,** 1742–1750.

Eng, P. H. K., Cardona, G. R., Fang, S., Previti, M., Alex, S., Carrasco, N., Chin, W. W., and Braverman, L. E. (1999). Escape from the acute Wolff-Chaikoff effect is associated with a decrease in thyroid sodium/iodide symporter messenger ribonucleic acid and protein. *Endocrinology* **140,** 3404–3410.

Escobar-Morreale, H. F., Escobar del Rey, F., Obregon, M. J., and Morreale de Escobar, G. (1996). Only the combined treatment with thyroxine and triiodothyronine ensures euthyroidism in all tissues of the thyroidectomized rat. *Endocrinology* **137,** 2490–2502.

Fail, P. A., Anderson, S. A., and Friedman, M. A. (1999). Response of the pituitary and thyroid to tropic hormones in Sprague-Dawley versus Fisher 344 male rats. *Toxicol. Sci.* **52,** 107–121.

Fukuda, H., Yasuda, N., Greer, M. A., Kutas, M., and Greer, S. E. (1975). Changes in plasma thyroxine, triiodothyronine, and TSH during adaptation to iodine deficiency in the rat. *Endocrinology* **97,** 307–314.

Gluzman, B. E., and Niepomniszcze, H. (1983). Kinetics of iodide trapping mechanism in normal and pathological human thyroid slices. *Acta Endocrinol.* **103,** 34–39.

Greer, M. A., Goodman, G., Pleus, R. C., and Greer, S. E. (2002). Health effects assessment for environmental perchlorate contamination: The dose response for inhibition of thyroidal radioiodine uptake in humans. *Environ. Health Perspect.* **110,** 927–937.

Greer, M. A., Grimm, Y., and Studer, H. (1968). Qualitative changes in the secretion of thyroid hormones induced by iodine deficiency. *Endocrinology* **83,** 1193–1198.

Gustafson, D. L., Rastatter, J. C., Colombo, T., and Long, M. E. (2002). Doxorubicin pharmacokinetics: Macromolecule binding, metabolism, and excretion in the context of a physiologic model. *J. Pharm. Sci.* **91,** 1488–1501.

Janssen, K., van der Heide, D., Visser, T. J., Kaptein, E., and Beynen, A. C. (1994). Thyroid function and deiodinase activities in rats with marginal iodine deficiency. *Biol. Trace. Elem. Res.* **40,** 237–246.

Kogai, T., Curcio, F., Hyman, S., Cornford, E. M., Brent, G. A., and Hershman, J. M. (2000). Induction of follicle formation in long-term cultured normal human thyroid cells treated with thyrotropin stimulates iodide uptake but not sodium/iodide symporter messenger RNA and protein expression. *J. Endocrinol.* **167,** 125–135.

Kogai, T., Endo, T., Saito, T., Miyazaki, A., Kawaguchi, A., and Onaya, T. (1997). Regulation by thyroid-stimulating hormone of sodium/iodide symporter gene expression and protein levels in FRTL-5 cells. *Endocrinology* **138,** 2227–2232.

Kogai, T., Taki, K., and Brent, G. A. (2006). Enhancement of sodium/iodide symporter expression in thyroid and breast cancer cells. *Endocrine-Related Cancer* **13,** 797–826.

Kohn, M. C., Sewall, C. H., Lucier, G. W., and Portier, C. J. (1996). A mechanistic model of effects of dioxin on thyroid hormones in the rat. *Toxicol. Appl. Pharmacol.* **165,** 29–48.

Krenning, E., Docter, R., Bernard, B., Visser, T., and Hennemann, G. (1981). Characteristics of active transport of thyroid hormone into rat hepatocytes. *Biochimica et Biophysica Acta.* **676,** 314–320.

Lemarchand-Beraud, T., and Berthier, C. (1981). Effects of graded doses of triiodothyronine on TSH synthesis and secretion rates in hypothyroid rats. *Acta Endocrinol.* **97,** 74–84.

Leonard, J. L., and Visser, T. J. (1986). Biochemistry of Deiodination. In *Thyroid Hormone Metabolism* (G. Hennemann, Ed.), pp. 189–229. Marcel Dekker, Inc., New York.

Levy, O., Dai, G., Riedel, C., Ginter, C. S., Paul, E. M., Lebowitz, A. N., and Carrasco, N. (1997). Characterization of the thyroid Na+/I- symporter with an anti-COOH terminus antibody. *Proc. Natl. Acad. Sci. USA.* **94,** 5568–5573.

Li, G., Liu, B., and Liu, Y. (1995). A dynamical model of the pulsatile secretion of the hypothalamic-pituitary-thyroid axis. *Biosystems* **35,** 83–92.

Malendowicz, L. K., and Bednarek, J. (1986). Sex dimorphism in the thyroid gland IV. Cytologic aspects of sex dimorphism in the rat thyroid gland. *Acta Anat.* **127,** 115–118.

McLanahan, E. D., Campbell, Jr., J. L., Ferguson, D. C., Harmon, B., Hedge, J. M., Crofton, K. M., Mattie, D. R., Braverman, L., Keys, D. A., Mumtaz, M., *et al.* (2007). Low-dose effects of ammonium perchlorate on the hypothalamic-pituitary-thyroid (HPT) axis of adult male rats pretreated with PCB126. *Toxicol. Sci.* **97,** 308–317.

Mendel, C. M., Cavalieri, R. R., and Kohrle, J. (1992). Thyroxine (T_4) transport and distribution in rats treated with EMD 21388, a synthetic flavonoid that displaces T_4 from transthyretin. *Endocrinology* **130,** 1525–1532.

Merrill, E. A., Clewell, R. A., Gearhart, J. M., Robinson, P. J., Sterner, T. R., Yu, K. O., Mattie, D. R., and Fisher, J. W. (2003). PBPK predictions of perchlorate distribution and its effect on thyroid uptake of radioiodide in the male rat. *Toxicol. Sci.* **73,** 256–269.

Merrill, E. A., Clewell, R. A., Sterner, T. R., and Fisher, J. W. (2005). PBPK model for radioactive iodide and perchlorate kinetics and perchlorate-induced inhibition of iodide uptake in humans. *Toxicol. Sci.* **83,** 25–43.

Michalkiewicz, M., Huffman, L. J., Connors, J. M., and Hedge, G. A. (1989). Alterations in thyroid blood flow induced by varying levels of iodine intake in the rat. *Endocrinology* **125,** 54–60.

Mirfazaelian, A., Kim, K., Lee, S., Kim, H. J., Bruckner, J. V., and Fisher, J. W. (2007). Organ growth functions in maturing male Sprague-Dawley rats. *J. Toxicol. Environ. Health A* **70,** 429–438.

Morreale de Escobar, G., Calvo, R., Escobar del Rey, F., and Obregon, M. J. (1994). Thyroid hormones in tissues from fetal an adult rats. *Endocrinology* **134,** 2410–2415.

Mukhopadhyay, B., and Bhattacharyya, R. (2006). A mathematical model describing the thyroid-pituitary axis with time delays in hormone transportation. *Appl. Math.* **51,** 549–564.

Naeije, R., Vanhaelst, L., and Golstein, J. (1978). Pituitary-thyroid axis during short term, mild and severe, iodine depletion in the rat. *Horm. Metab. Res.* **10,** 521–525.

Nguyen, T. T., DiStefano, III, J. J., Yamada, H., and Yen, Y. M. (1993). Steady state organ distribution and metabolism of thyroxine and 3,5,3′-triiodothyronine in intestines, liver, kidneys, blood, and residual carcass of the rat in vivo. *Endocrinology* **133,** 2973–2983.

Obregon, M., Escobar del Rey, F., and Morreale de Escobar, G. (2005). The effects of iodine deficiency on thyroid hormone deiodination. *Thyroid* **15,** 917–929.

Okamura, K., Taurog, A., and Krulich, L. (1981a). Strain differences among rats in response to Remington iodine-deficient diets. *Endocrinology* **109,** 458–463.

Okamura, K., Taurog, A., and Krulich, L. (1981b). Elevation of serum 3,5,3′-triiodothyronine and thyroxine levels in rats fed Remington diets; opposing effects of nutritional deficiency and iodine deficiency. *Endocrinology* **108,** 1247–1256.

Pedraza, P. E., Obregon, M., Escobar-Morreale, H. F., Escobar del Rey, F., and Morreale de Escobar, G. (2006). Mechanisms of adaptation to iodine deficiency in rats: Thyroid status is tissue specific. Its relevance for man. *Endocrinology* **147,** 2098–2108.

Rasgon, N. L., Pumphrey, L., Prolo, P., Elman, S., Negrao, A. B., Licinio, J., and Garfinkel, A. (2003). Emergent oscillations in mathematical model of the human menstrual cycle. *CNS Spectr.* **8,** 805–814.

Riedel, C., Levy, O., and Carrasco, N. (2001). Post-transcriptional regulation of the sodium/iodide symporter by thyrotropin. *J. Biol. Chem.* **276,** 21458–21463.

Riesco, G., Taurog, A., Larsen, P. R., and Krulich, L. (1977). Acute and chronic responses to iodine deficiency in rats. *Endocrinology* **100,** 303–313.

Rutgers, M., Pigmans, I. G., Bonthuis, F., Docter, R., and Visser, T. J. (1989). Effects of propylthiouracil on the biliary clearance of thyroxine (T_4) in rats: Decreased excretion of 3,5,3′-triiodothyronine glucuronide and increased excretion of 3,3′,5′-triiodothyronine glucuronide and T_4 sulfate. *Endocrinology* **125,** 2175–2186.

Schlosser, P. M., and Selgrade, J. F. (2000). A model of gonadotropin regulation during the menstrual cycle in women: Qualitative features. *Environ. Health Perspect.* **108,** 873–881.

Sherwin, J. R., and Tong, W. (1974). The actions of iodide and TSH on thyroid cells showing a dual control system for the iodide pump. *Endocrinology* **94,** 1465–1474.

Siglin, J. C., Mattie, D. R., Dodd, D. E., Hildebrandt, P. K., and Baker, W. H. (2000). A 90-day drinking water toxicity study in rats of the environmental contaminant ammonium perchlorate. *Toxicol. Sci.* **57,** 61–74.

Simpkins, J. W., Bruni, J. F., Mioduszewski, R. J., and Meites, J. (1976). Serum and pituitary TSH and response to TRH in developing male and female rats. *Endocrinology* **98,** 1365–1369.

Téllez, R. T., Chacón, P. M., Abarca, C. R., Blount, B. C., Van Landingham, C. B., Crump, K. S., and Gibbs, J. P. (2005). Long-term environmental exposure to perchlorate through drinking water and thyroid function during pregnancy and the neonatal period. *Thyroid* **15,** 963–975.

Tonacchera, M., Pinchera, A., Dimida, A., Ferrarini, E., Agretti, P., Vitti, P., Santini, F., Crump, K., and Gibbs, J. (2004). Relative potencies and additivity of perchlorate, thiocyanate, nitrate, and iodide on the inhibition of radioactive iodide uptake by the human sodium iodide symporter. *Thyroid* **14,** 1012–1019.

Tornero-Velez, R., and Rappaport, S. M. (2001). Physiological modeling of the relative contributions of styrene-7,9-oxide derived from direct inhalation and from styrene metabolism to the systemic dose in humans. *Toxicol. Sci.* **64,** 151–161.

Verger, P., Aurengo, A., Geoffroy, B., and Le Guen, B. (2001). Iodine kinetics and effectiveness of stable iodine prophylaxis after intake of radioactive iodine: A review. *Thyroid* **11,** 353–360.

Visser, T. J., Kaptein, E., van Toor, H., van Raaij, J. A. G. M., van den Berg, K. J., Joe, C. T. T., van Engelen, J. G. M., and Brouwer, A. (1993). Glucuronidation of thyroid hormone in rat liver: Effects of *in vivo* treatment with microsomal enzyme inducers and *in vitro* assay conditions. *Endocrinology* **133,** 2177–2186.

Visser, T. J., van Buuren, J. C. J., Rutgers, M., Rooda, S. J. E., and de Herder, W. W. (1990). The role of sulfation in thyroid hormone metabolism. *Trends Endorcinol. Metab.* **1,** 211–218.

Yu, K. O., Narayanan, L., Mattie, D. R., Godfrey, R. J., Todd, P. N., Sterner, T. R., Mahle, D. A., Lumpkin, M. H., and Fisher, J. W. (2002). The pharmacokinetics of perchlorate and its effect on the hypothalamus-pituitary-thyroid axis in the male rat. *Toxicol. Appl. Pharmacol.* **182,** 148–159.

Zoeller, R. T. (2007). Environmental chemicals impacting the thyroid: Targets and consequences. *Thyroid* **17,** 811–817.

Zoeller, R. T., and Tan, S. W. (2007). Implications of research on assays to characterize thyroid toxicants. *Crit. Rev. Toxicol.* **37,** 195–210.